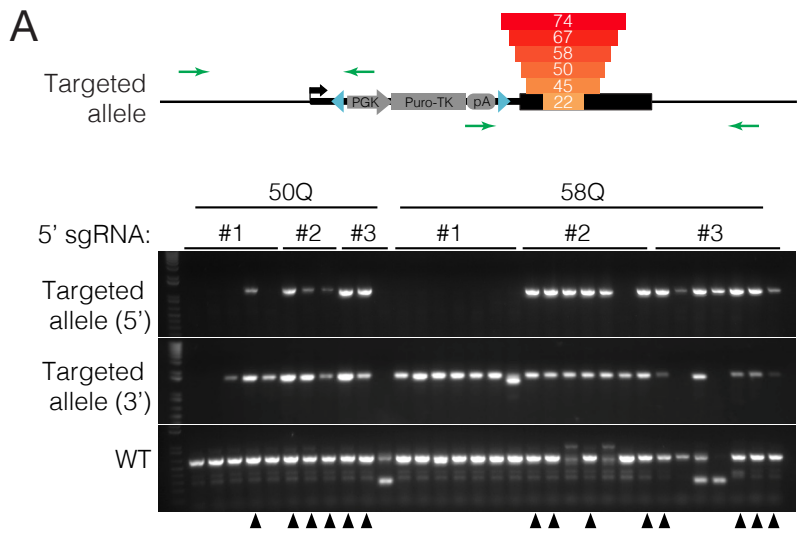
A
Targeted allele
74
67
58
50
45
22
PGK
Puro-TK
pA
50Q
58Q
5' sgRNA:
#1
#2
#3
#1
#2
#3
Targeted allele (5')
Targeted allele (3')
WT

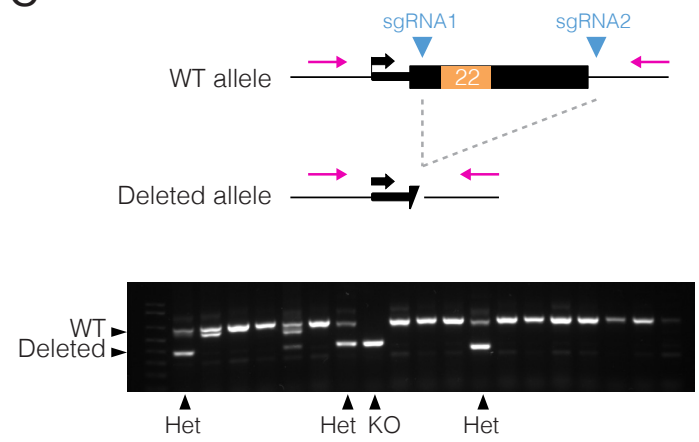
C
sgRNA1
sgRNA2
WT allele
22
Deleted allele
WT
Deleted
Het
Het
KO
Het

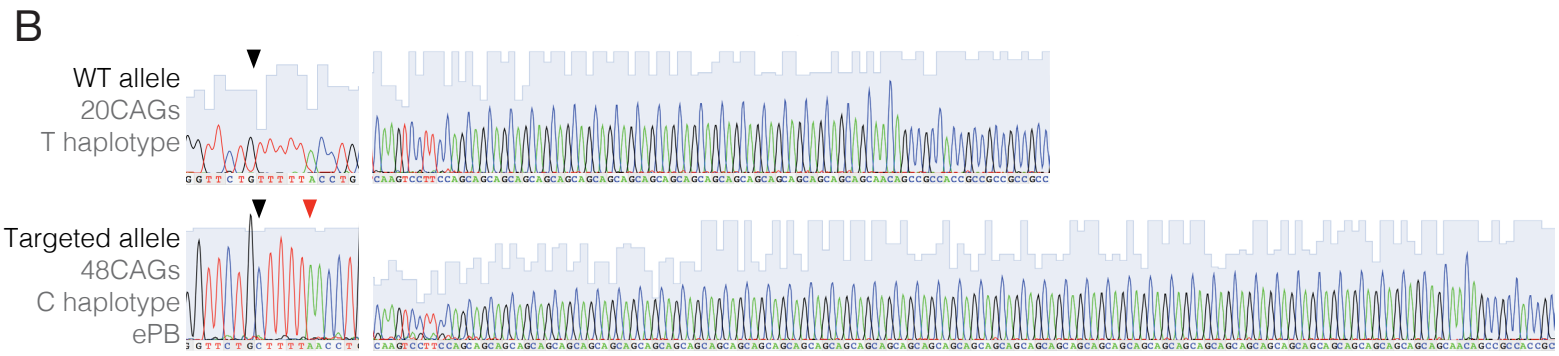
B
WT allele
20CAGs
T haplotype
Targeted allele
48CAGs
C haplotype
ePB

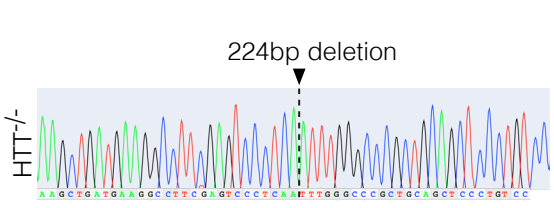
D
224bp deletion
HTT-/-

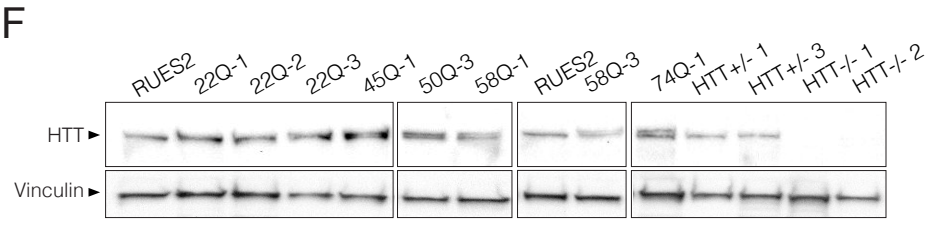
F
RUES2
22Q-1
22Q-2
22Q-3
45Q-1
50Q-3
58Q-1
RUES2
58Q-3
74Q-1
HTT+/- 1
HTT+/- 3
HTT-/- 1
HTT-/- 2
HTT
Vinculin

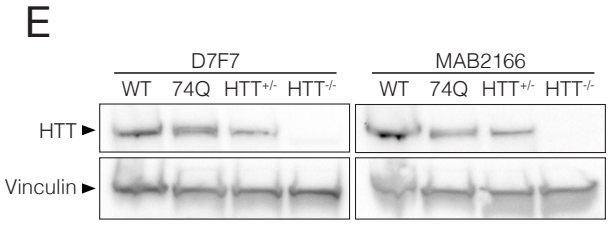
E
D7F7
MAB2166
WT
74Q
HTT+/-
HTT-/-
WT
74Q
HTT+/-
HTT-/-
HTT
Vinculin

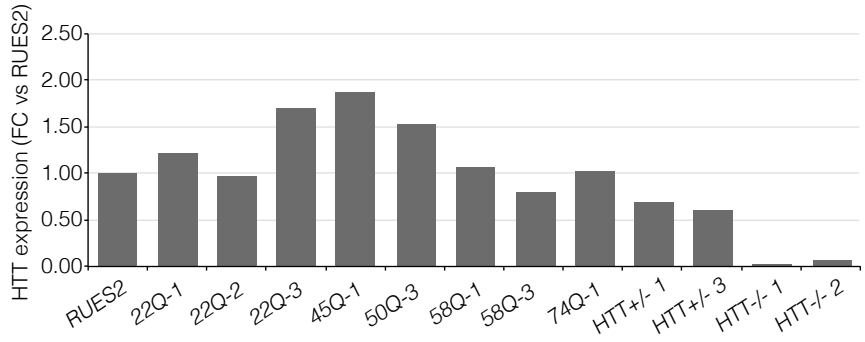
HTT expression (FC vs RUES2)
2.50
2.00
1.50
1.00
0.50
0.00
RUES2
22Q-1
22Q-2
22Q-3
45Q-1
50Q-3
58Q-1
58Q-3
74Q-1
HTT+/- 1
HTT+/- 3
HTT-/- 1
HTT-/- 2

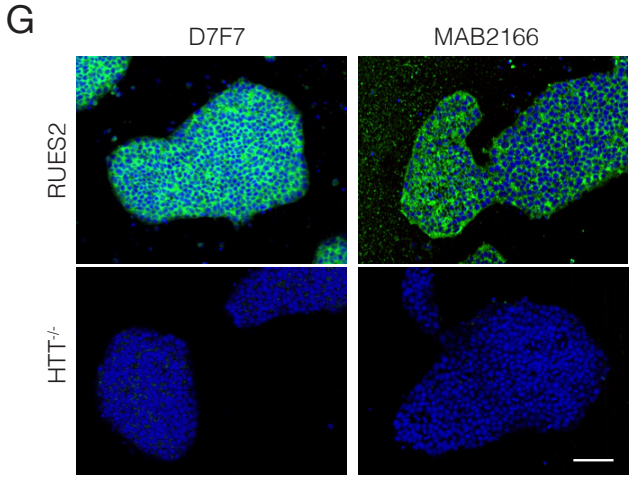
G
D7F7
MAB2166
RUES2
HTT-/-

Figure S1. Validation of the HD-hESC allelic series. (A) PCR screening of HD-hESC targeted clones after CRISPR/Cas9-mediated homologous recombination. Primers flanking the 5' and 3' arms were used to detect targeted alleles. A primer pair that amplifies the WT was also used to identify heterozygotically vs homozygotically targeted clones. (B) Sanger sequencing example of both the targeted and untargeted allele in one of the 50Q targeted clones. The convenient location of a heterozygotic SNP allowed for the identification of which of the two alleles was targeted. (C) PCR screening of targeted clones after CRISPR/Cas9-mediated HTT exon 1 deletion. Primers flanking the deleted region were used to detect targeted alleles. (D) Sanger sequencing example of the deleted alleles in a $HTT^{-/-}$ line. (E) Expression of both expanded and wildtype HTT protein is detected in RUES2-74Q, while it is absent in $HTT^{-/-}$ clones and reduced in $HTT^{+/-}$ clones. Western Blot using two independent HTT antibodies: D7F7 and MAB2166. (F) Western Blot using MAB2166 antibody for multiple genotypes and sub-clones, and the appropriate quantification below. HTT expression is variable between genotypes and clones, but consistently decreased at ~60% in the heterozygous clones. (G) Comparison of the HTT subcellular localization in pluripotency conditions by IF using two independent antibodies: D7F7 and MAB2166. Both antibodies provide a cytoplasmic signal, which is clearly excluded from the nucleus. Scale bar 25μm.

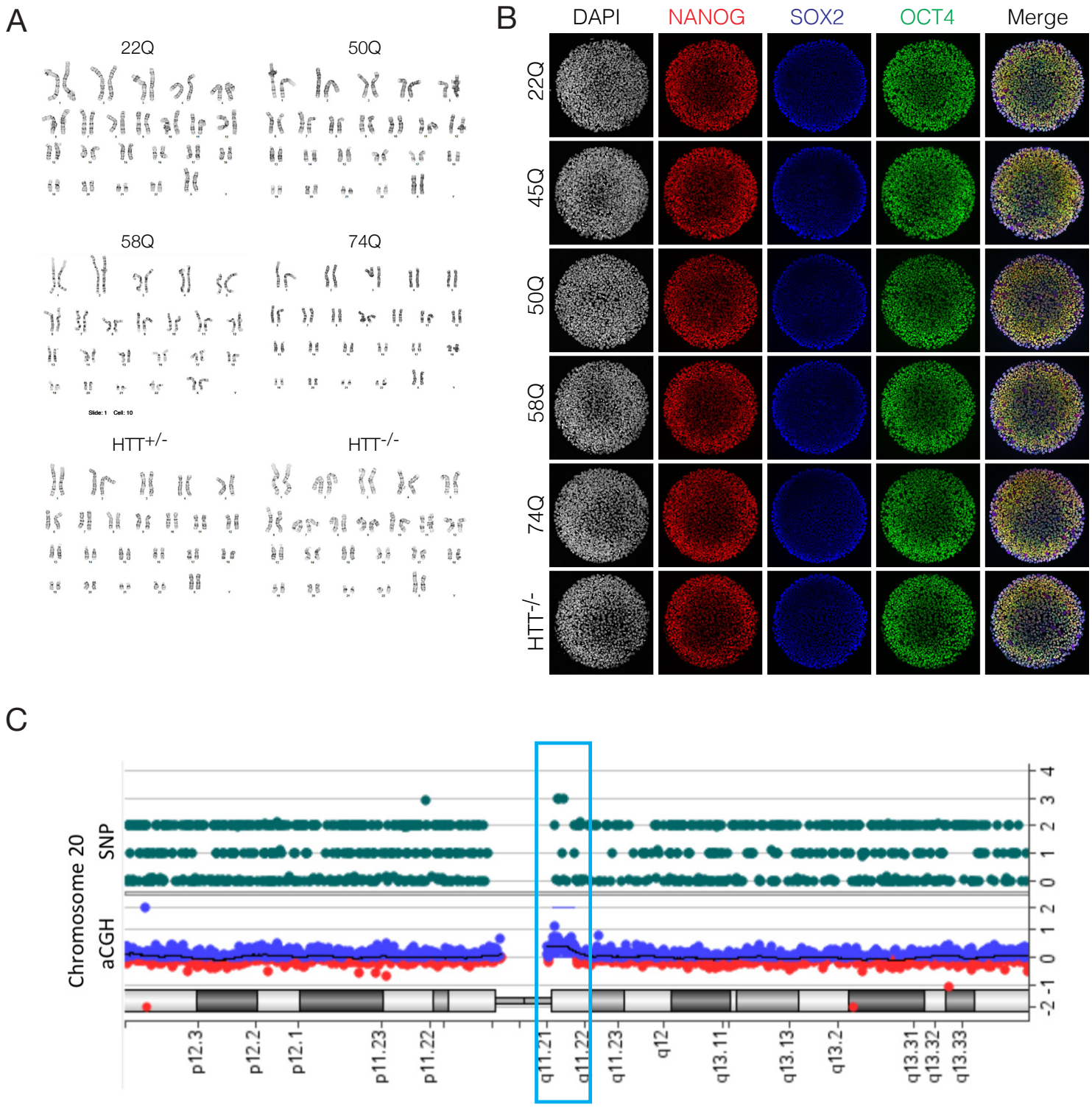

Figure S2. Karyotyping and pluripotency validation of the HD-hESC allelic series
(A) All hESC isogenic clones were karyotypically normal by G-banding. (B) The pluripotency status was not affected by the length of the polyQ tract or the HTT dosage. Immunostaining of micropatterned hESC cultures for pluripotency markers NANOG, SOX2 and OCT4. Scale bar 100µm. (C) Example of aCGH analysis result (amplification of 20q11). aCGH analyses revealed different CNVs present in different sub-clones.

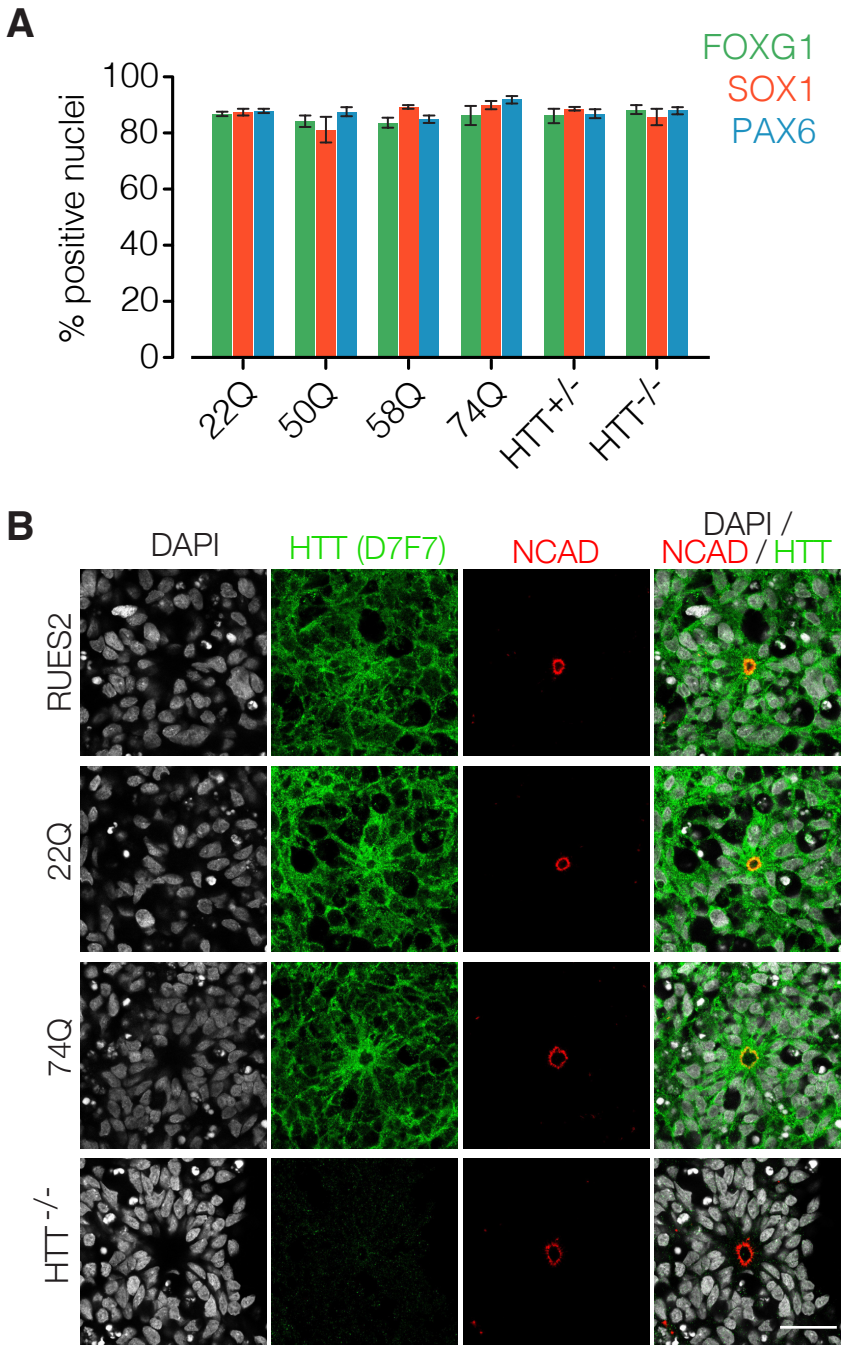

Figure S3. Neural rosette differentiation and impairment of inter-rosette self-organization in expanded polyQ and HTT$^{-/-}$ lines. (A) Neural induction and positional identity were unaffected by polyQ length or HTT dosage. Mean % of all DAPI nuclei positive for SOX1, PAX6, FOXG1, +/- SEM, n=2-3 lines/genotype, >2000 cells scored per line. (B) Full-length HTT protein localized to the cytoplasm in neural progenitors at neural rosette stage and its intracellular localization is not affected by the increasing polyQ lengths. Immunostaining for DNA (DAPI, white), HTT (D7F7, green), and NCADHERIN (red), 40x confocal z-section, Scale Bar 50μm. (C) Immunostaining for DNA (DAPI, white) and HTT (MAB2166, green) in neural progenitors at neural rosette stage, confirming the HTT subcellular localization detected with D7F7 antibody. (D) Representative immunostainings of NCAD foci for 22Q and 58Q lines, and their corresponding locations after image processing. (E) Cumulative distributions of the nearest neighbor distances of individual lines, and combined, compared to the one expected from a random arrangement of rosettes (black dashed line).

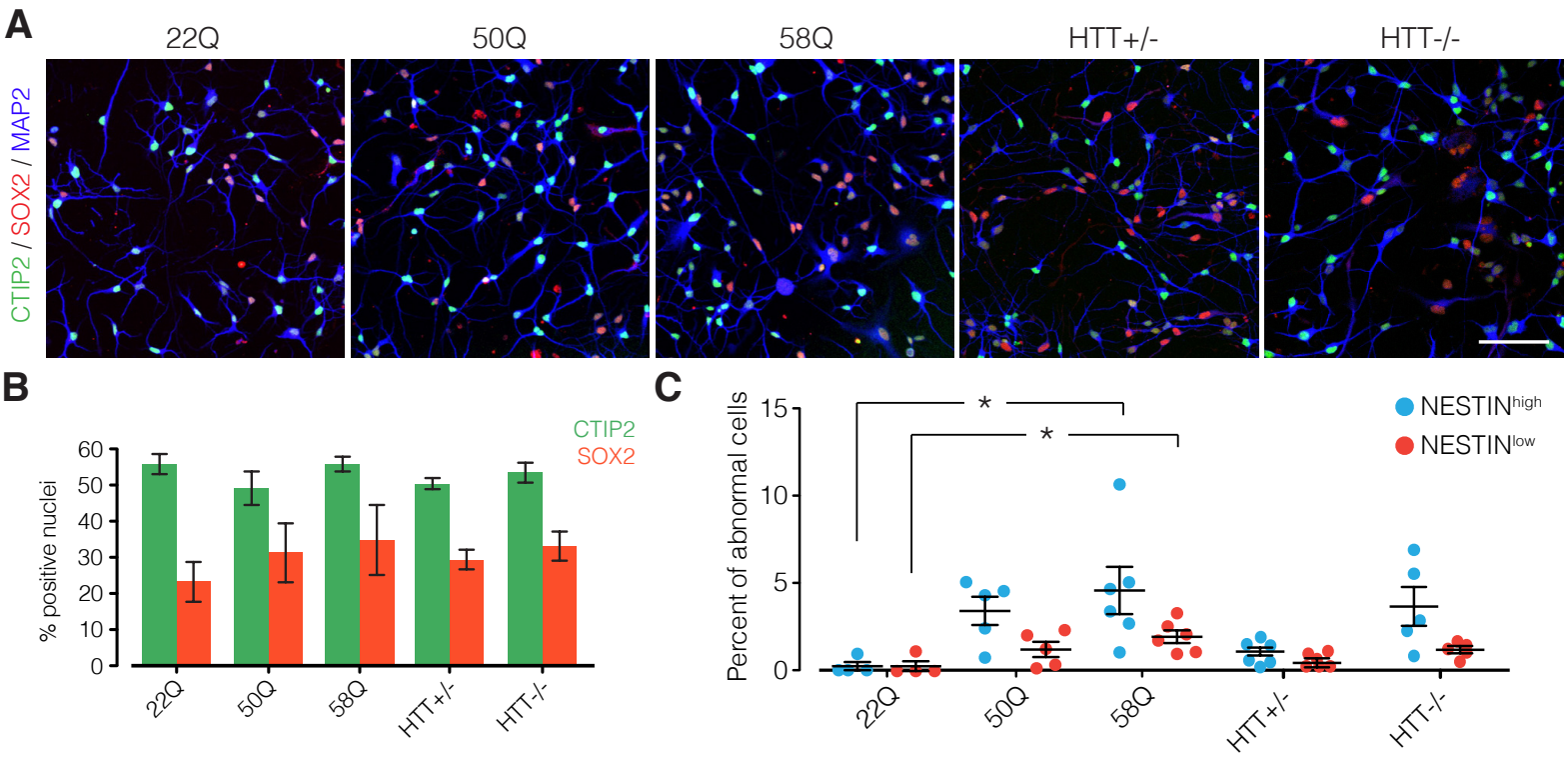
A
22Q
50Q
58Q
HTT+/-
HTT-/-
CTIP2 / SOX2 / MAP2
B
CTIP2
SOX2
% positive nuclei
22Q
50Q
58Q
HTT+/-
HTT-/-
C
NESTIN^high
NESTIN^low
Percent of abnormal cells
*
*
D
d0
22Q
50Q
58Q
74Q
43Q
50Q
58Q
HTT-/-
HTT+/-
RUES2
58Q-1
d22
d40
HTT ►
Vinculin ►
E
Intensity (a.u.)
Linescan distance (um)
F
Allelic expression ratio (expanded vs WT)
Days of neural differentiation
45Q-1
45Q-3
50Q-2
50Q-3
58Q-1
58Q-3
72Q-1
Mean +/- SD

Figure S4. Isogenic HD hESC lines are able to differentiate to post-mitotic neurons, but display morphological phenotypes. (A-B) At day 45, cultures are composed of post-mitotic neurons (A) staining for ($MAP2^+$, blue) and cortical neuronal marker CTIP2, and SOX2+ (red) $NESTIN^+$ (not shown) progenitor cells , 20x confocal z stack maximum intensity projection with (B) no significant difference in abundance between genotypes. Mean % of DAPI +/- SEM of n=2-3 independent lines per genotype, >1000 cells scored per line. Scale bar 50um. (C) Quantification of the frequency of abnormal cells, classified by phenotype as progenitors ($Nestin^{high}$), or post-mitotic neurons ($Nestin^{low}$). * p-value <0.05 in an ANOVA test. (D-F) HTT allelic expression analysis along neuronal differentiation. (D) Western Blot of representative clones for multiple genotypes at either day 22 or 40 of neuronal differentiation. (E) Example of the method of quantification of the differential allelic expression. (F) Both the expanded and the wildtype allele were expressed at approximately the same levels (ratio expanded vs wildtype ~ 1.1).

Table S1. Analysis of whole genome sequence data from HD allelic lines. No mutations were observed in any of the lines at any of the predicted off-target loci for any of the sgRNAs used in the generation of the lines.

Sample	# of SNP variants in whole genome (compared to hg19)	# of new SNP Variants in whole genome (compared to RUES2)	# of unique new SNP Variants in whole genome (compared to rest of lines)	# *de novo* Variants near predicted sgRNA25 off-targets	# *de novo* Variants near predicted sgRNA14 off-targets	# *de novo* Variants near predicted sgRNA22 off-targets
RUES2 (parental)	4,405,573	N/A	N/A	N/A	N/A	N/A
22Q-1	4,401,985	1,364	1,256	0	0	0
50Q-1	4,416,582	1,491	1,203	0	0	0
50Q-2	4,417,218	2,063	1,934	0	0	0
50Q-3	4,416,294	1,737	1,608	0	0	0
58Q-1	4,413,149	1,346	1,047	0	0	0
58Q-2	4,419,108	1,601	1,394	0	0	0
58Q-3	4,417,117	1,311	1,005	0	0	0
HTT+/- 1	4,416,777	1,376	1,215	0	0	0
HTT+/- 2	4,416,560	958	656	0	0	0
HTT+/- 3	4,402,404	733	466	0	0	0
HTT-/- 1	4,417,789	1,185	893	0	0	0

Table S2. Summary of Arrayed Comparative Genomic Hybridization (aCGH) analysis to assess copy number variations in the RUES2-HD allelic series. We found a variety of copy number variations and loss-of-heterozygosity, within and outside of normal ranges, but these did not correlate with any of the observed phenotypic differences.

Color Legend
AMP
DEL
LOH

Cell line	1	2	3	4	5	6	7	8	9	10	11	12	13	14	15	16	17	18	19	20	21	22	X
22Q-1		p12 - p11.2 q13 q34		p16.3						q23.32									q13.2-q13.31	q11.21			
22Q-2		p12 - p11.2 q13		p16.3	q21.3 - q22.1					q23.32				q32.33				q22.1 - q23	q13.2-q13.31				
22Q-3		p12 - p11.2 q13		p16.3	q21.3 - q22.1		q36.2			q23.32							q12 - q21.31		q13.2-q13.31	q11.21			
45Q-1		p12 - p11.2 q13			q21.3 - q22.1					q23.32							q12 - q21.31		q13.2-q13.31				
50Q-1		p12 - p11.2 q13 q14.2		p16.3	q21.3 - q22.1					q23.32				q32.33			q12 - q21.31						
50Q-2		p12 - p11.2 q13			q21.3 - q22.1					q23.32				q32.33			q12 - q21.31						
50Q-3		p12 - p11.2 q13		p16.3	q21.3 - q22.1					q23.32		q12.3							q13.2-q13.31				
58Q-1		p12 - p11.2 q13		p16.3	q21.3 - q22.1					q23.32					q11.1 - q11.2								q22.1-q22.2
58Q-2		p12 - p11.2 q13		p16.3	q21.3 - q22.1		q12.1-p11.2			q23.32				q32.33					q13.2-q13.31				
58Q-3		p12 - p11.2 q13		p16.3	q21.3 - q22.1					q23.32				q32.33			q12 - q21.31		q13.2-q13.31				q22.1-q22.2
67Q-1		p12 - p11.2 q13		p16.3	q21.3 - q22.1		q31.32			q23.32				q32.33					q13.2-q13.31				
74Q-1		p12 - p11.2 q13		p16.3	q21.3 - q22.1					q23.32				q32.33					q13.2-q13.31	q11.21			
74Q-2		p12 - p11.2 q13 q34		p16.3	q21.3 - q22.1	q22.31				q23.32				q32.33			q12 - q21.31		q13.2-q13.31	q11.21			
HTT+/- 1		p12 - p11.2 q13		p16.3	q21.3 - q22.1					q23.32				q32.33			q12 - q21.31		q13.2-q13.31				q22.1-q22.2
HTT+/- 2		p12 - p11.2 q13		p16.3	q21.3 - q22.1		q31.32			q23.32				q32.33			q12 - q21.31		q13.2-q13.31				q22.1-q22.2
HTT+/- 3		p12 - p11.2 q13		p16.3	q21.3 - q22.1					q23.32										q11.21			
HTT-/- 1		q13		p16.3	q21.3 - q22.1					q23.32				q32.33						q11.21			
HTT-/- 2		p12 - p11.2 q13		p16.3	q21.3 - q22.1				q33.1	q23.32							q12 - q21.31			q11.21			
HTT-/- 3		p12 - p11.2 q13		p16.3	q21.3 - q22.1					q23.32				q32.33			q12 - q21.31			q11.21			

RUES2 parental stock 1		p12 - p11.2 q13		p16.3	q21.3 - q22.1					q23.32				q32.32			q12 - q21.31		q13.2-q13.31				
RUES2 parental stock 2		p12 - p11.2 q13		p16.3	q21.3 - q22.1					q23.32				q32.33					q13.2-q13.31				
RUES2 parental stock 3		p12 - p11.2 q13		p16.3	q21.3 - q22.1					q23.32							q12 - q21.31		q13.2-q13.31				

Table S3. Primers

Fragment	Fw primer sequence	Rv primer sequence	Template
pUC57-Kan bb	CTCCAGCTTTTGTTCCCTTT	CCAATTCGCCCTATAGTGAGTC	pUC57-Kan plasmid
Left homology arm	AAAGGGAACAAAAGCTGGAGgggtcacacttggggtcct	TCTAGGGTTAAaagcagaacctgagcggc	gDNA from RUES2 (WT)
ePB-PUTK	aggttctgcttTTAACCCTAGAAAGATAGTCTGC	GGGCCGCAGGTTAACCCTAGAAAGATAATCATATTG	ePB-CAG-PUTK-pA plasmid
Right homology arm	TTTCTAGGGTTAACCTGCGGCCCAGAGCCC	GACTCACTATAGGGCGAATTGGCCTCCCCATCAGCAACGTGT	gDNA from RUES2 (WT)

Table S4. Templates used for each CAG length.

polyQ length	Origin of genomic DNA template	Obtained from
44	ND38548 iPSC	Coriell Biorepository
50	GENEA20 hESC	GENEA
58	QS-001 fibroblasts	Tabrizi lab
69	QS-004 fibroblasts	Tabrizi lab
75	QS-004 fibroblasts	Tabrizi lab

Table S5. sgRNAs

sgRNA	Protospacer + PAM sequence
hHTT_sgRNA25	GGTAAAAGCAGAACCTGAG CGG
hHTT_sgRNA22	CTGCTGCTGGAAGGACTTGA GGG
hHTT_sgRNA14	GCTGCACCGACCGTGAGTTT GGG

Table S6. Antibodies

Name	Supplier	Catalog number	Dilution Factor
PAX6	Covance	PRB-278	200
PAX6	BD Biosciences	561462	200
SOX1	R&D	AF3369	1000
NES	EMD Millipore	ABD69	500
FOXG1	Abcam	ab18259	200
HTT (D7F7)	Cell Signaling	5656S	100
N-cadherin	BioLegend	350802	100
Acetylated tubulin	Sigma-Aldrich	T-6793	200
Pericentrin	Abcam	ab28144	200
SOX2	R&D	AF2018	1000
CTIP2	Abcam	ab18465	200
MAP2	Abcam	ab5392	5000
Aurora b kinase	Abcam	ab2254	100
Alpha-tubulin	Abcam	ab89984	500
CREST	Antibodies Incorporated	15-235-0001	100

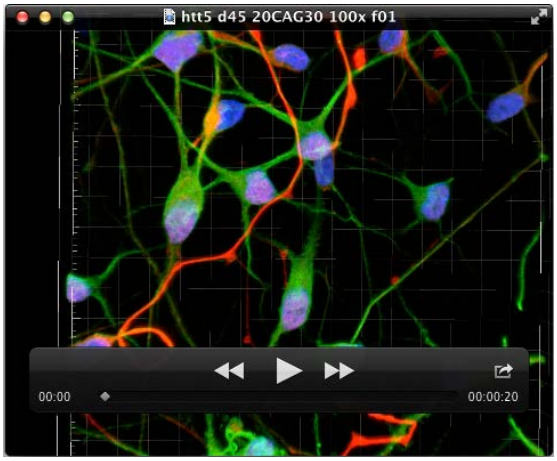

Movie 1. Three-dimensional Imaris rendering of deconvolved 100x confocal z-stack of a normal day 45 neuronal culture of RUES2-22Q stained for MAP2 (green), CTIP2 (purple), nestin (red), and DAPI (blue). Note the thin processes, and the absence of multi-nucleated cells.

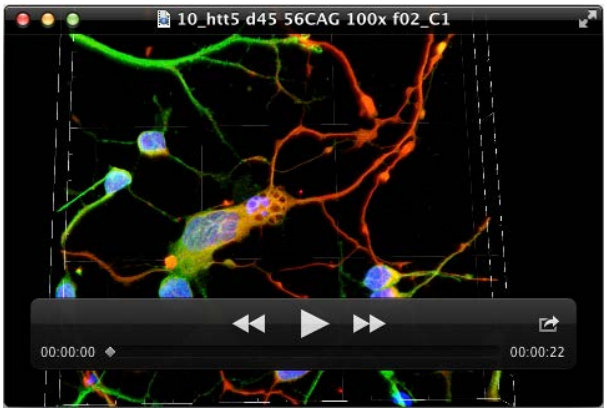

Movie 2. Three-dimensional rendering of 100x confocal z-stack of an abnormal progenitor cell in RUES2-58Q cultures after 45 days of neuronal differentiation, stained for MAP2 (green), CTIP2 (purple), nestin (red), and DAPI (blue). Note the abnormal progenitor cell in the center with an enlarged soma, displaying multiple separated nuclei, thicker processes, enlarged vacuoles and a co-expression of nestin and MAP2 markers.

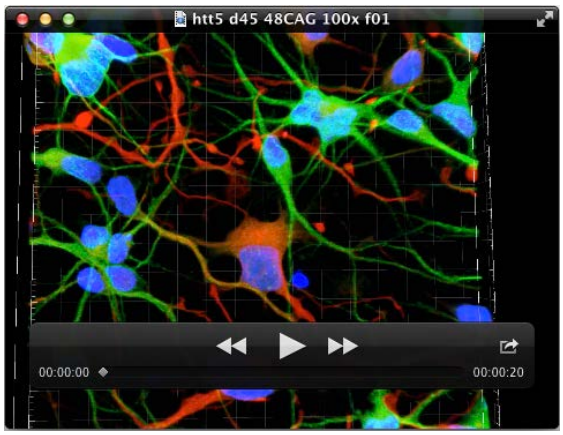

Movie 3. Three-dimensional rendering of 100x confocal z-stack of abnormal post-mitotic neurons in RUES2-50Q cultures after 45 days of neuronal differentiation, stained for MAP2 (green), CTIP2 (purple), nestin (red), and DAPI (blue). Several multinucleated cells can be observed in the region, but of upmost interest is the cell in the top-right, which displays the typical phenotype of abnormal post-mitotic neurons: multiple nuclei linked together by strands of DNA, forming a 'nuclear bouquet'.

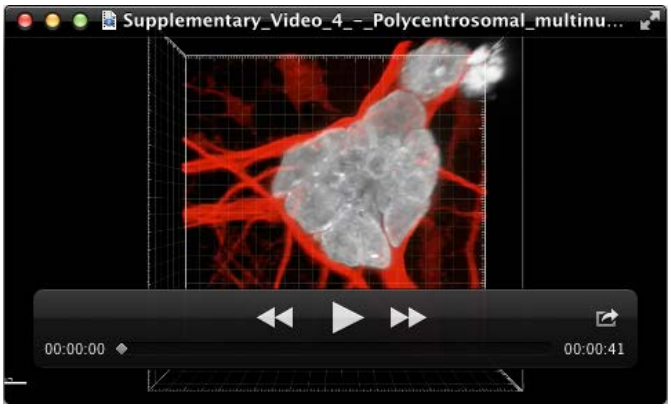

Movie 4. Three-dimensional rendering of 100x confocal z-stack of an abnormal post-mitotic neuron, showing typical nuclear bouquets containing multiple concentric centrosomes located close to the center of the nuclear bouquet, suggestive of strong polarity defects. Adjusted signal for all channels, acetylated tubulin (red), pericentrin (green) and DAPI (white) are shown, followed by surfaces-modeled by thresholding on intensity for DAPI and pericentrin.

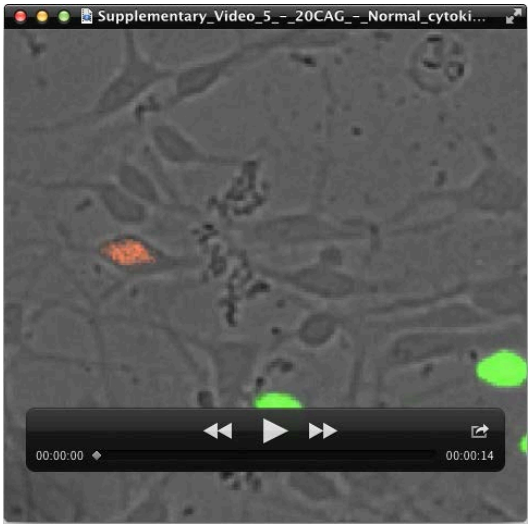

Movie 5. Time-lapse imaging of mixed RFP- and GFP-labeled RUES2-22Q cultures between days 28-31 of neuronal differentiation. Note two GFP-labeled daughter cells separate and move independently shortly after cell division.

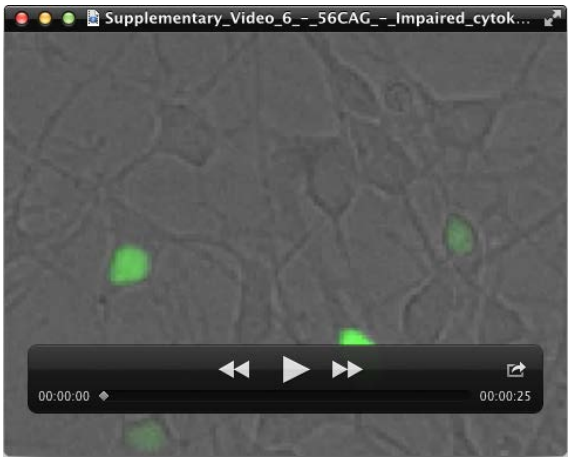

Movie 6. Time-lapse imaging of mixed RFP- and GFP-labeled RUES2-58Q cultures between days 28-31 of neuronal differentiation. Note two GFP-labeled daughter cells are unable to separate after cell division, and they come back together generating a multinucleated cell.

Movie 7. Time-lapse imaging of mixed RFP- and GFP-labeled RUES2-22Q cultures between days 28-31 of neuronal differentiation. Impaired cell divisions were observed in multiple consecutive rounds of karyokinesis, suggesting that once a multinucleated cell is generated, it cannot be resolved in successive cell divisions.

Movie 8. Three-dimensional rendering of an 100x confocal z-stack of a dividing cell with normal centromere counts (92) displaying lagging chromosomes in RUES2-58Q. DAPI, white; alpha-tubulin, red; CREST (centromere protein reactive serum), green. Scale bar, 5 μm.